Analysis, design and testing of a novel direct-drive wave energy converter system

ANALYSIS, DESIGN AND TESTING OF A NOVEL DIRECT-DRIVE WAVE ENERGY CONVERTER SYSTEM

R. Crozier*, *H. Bailey*, *E. Spooner*†, *P. McKeever*‡, *M.A. Mueller*

**Institute for Energy Systems, The University of Edinburgh, UK*
Email: r.crozier@ed.ac.uk, helen.bailey@ed.ac.uk, markus.mueller@ed.ac.uk.
†*EM Renewables ltd., UK, Email: ed.fieldstile@gmail.com*
‡*National Renewable Energy Centre ltd., UK, Email: paul.mckeever@narec.co.uk*

Keywords: wave energy, direct-drive, permanent magnet, snapper

Abstract

A coupled electromechanical and hydrodynamic simulation of a direct-drive generator connected to a heaving buoy for wave energy conversion has been developed. The system is based around a novel linear generator referred to as 'Snapper' which incorporates a magnetic coupling, resulting in a latching power take-off mechanism. The system has been simulated in the time domain using the Matlab differential equation solvers, and a prototype generator designed, built and tested.

1. Introduction

Wave energy has the potential to provide significant amounts of sustainable power if the associated engineering challenges of operating in the marine environment can be overcome whilst minimizing costs [9]. The cost of the inevitable repairs and maintenance throughout the lifetime of any Wave Energy Converter (WEC) remains a major difficulty. One proposed method of minimizing the required maintenance is the use of a system based around a direct-drive linear generator [12,13]. Several systems based around this technology have been both designed and implemented [14,16].

Typically, WECs operate at much lower velocities than the optimum speed of conventional generator technologies, and undergo high forces. Therefore, to achieve reasonable efficiencies, direct-drive generators tend to require large amounts of high coercivity permanent magnet material and, as a consequence, bulky structures to maintain the airgap against the Maxwell stresses induced by the intense magnetic field. Both of these requirements result in heavy and expensive machines which are difficult to construct and handle. Here a WEC is presented which consists of a point absorber, and a novel generator topology designed to alleviate some of these difficulties.

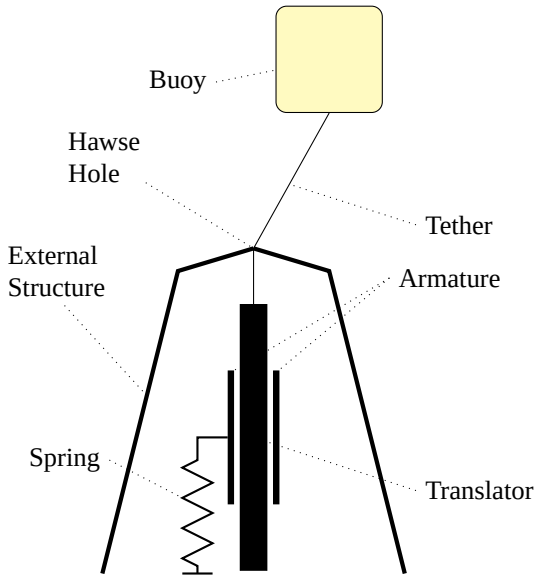

Fig. 1. Snapper wave energy converter conceptual system diagram. Note the two sides of the armature are rigidly connected out of plane.

2. The WEC

The WEC is made up of a heaving buoy attached via a tether to a direct-drive generator. A diagram of the arrangement is shown in Fig. 1. The Snapper generator consists of three parts, the armature, a set of springs attached between the armature and the sea bed fixing, and the translator which is attached to the heaving buoy. Other configurations are possible, but are not explored here. The armature consists of copper wire coils, steel for electrical purposes, some structural material and, unusually, magnets. The translator has a second series of permanent magnets mounted along it's length. The coils on the armature produce the electrical power when they move relative to the magnets on the translator. The faster this motion occurs, the smaller, and cheaper, the magnets and overall machine must be to achieve a reasonable power output. On both the armature and translator the magnets are mounted with alternating polarity as shown in Fig. 3.

As both the translator and armature have magnets mounted on them, the two parts are attracted to a stable configuration with the magnets on the armature and translator facing each

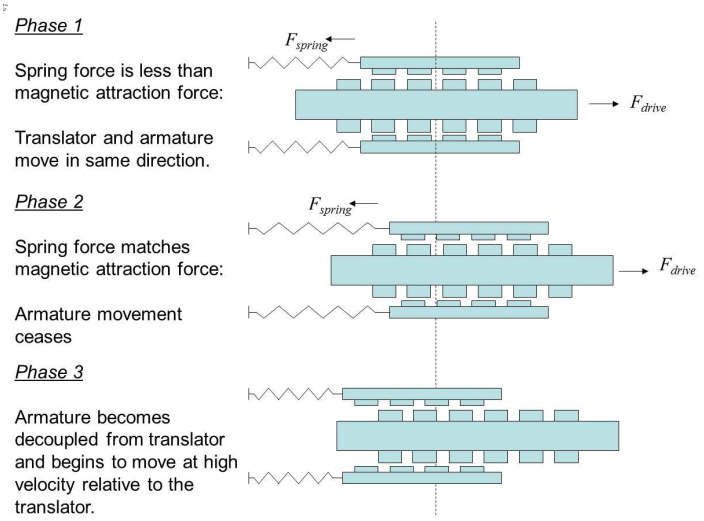

Fig. 2. Snapper system conceptual operation diagram.

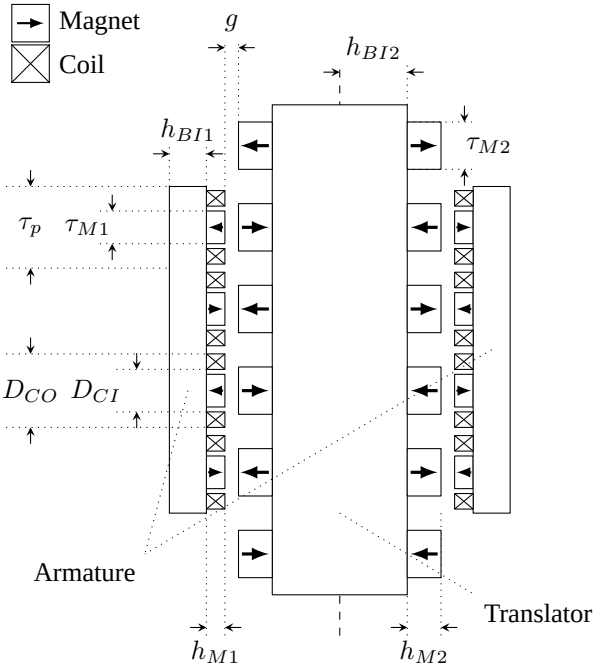

Fig. 3. Snapper cross-section diagram

other. When a force is applied to the translator, the armature is pulled along with it by the magnetic attraction. However as the armature is moved, the spring between it and the fixing point extends and applies a reverse force to the armature. Eventually the spring forces are sufficient to overcome the magnetic attraction, at which point the armature accelerates rapidly in the opposite direction to the translator movement. This high speed movement produces a pulse of power. In principle, this high speed movement should allow the reduction in size of the required magnets and their associated costs and also ease some of structural design problems resulting from the necessity for very high strength magnetic fields. The principle of operation is demonstrated graphically in Fig. 2.

2.1 The Electromechanical Model

The relative positions and velocities of the armature and translator are required to determine the flux linkage and resulting EMF generated in the coils during dynamic operation. The positions of the armature and translator relative to a global coordinate system are denoted x_A and x_T. The relative positions and velocities of the armature and translator, x_R and $\dot{x}_R$, are given by $x_T - x_A$ and $\dot{x}_T - \dot{x}_A$ respectively.

Within the machine, forces arise due to the interaction of the two sets of magnets, the electromagnetic damping forces due to the current carrying coils, and possibly other damping forces due to losses within the machine.

The most conventional method of simulating the electromagnetic forces and other quantities of interest, such as the flux linkage (λ) in the coils, while accounting for saturation and other nonlinearities, is to perform Finite Element Analysis (FEA). Unfortunately FEA is computationally intensive, and time-stepped FEA would be practically infeasible.

Therefore, to minimize the necessary computational time, a look-up table of the values of interest is compiled from FEA results at different values of relative positions (x_R) and coil current densities (J). Polynomials are then fitted to this data with the independent variables being x_R and J and the dependent variable being the output values of interest. The FEA was performed using FEMM [5], an open source, finite element analysis package.

The EMF produced in the coil is the rate of change of flux linkage with respect to time, which can be obtained from (1). The derivative of the flux linkage with respect to relative position, in the previous equation, is found by taking the numerical derivative of the polynomial fitted to the look-up table mentioned previously with respect to x_R, while holding J constant.

$$\text{EMF} = -\frac{\mathrm{d}\,\lambda}{\mathrm{d}\,t} = -\frac{\mathrm{d}\,\lambda}{\mathrm{d}\,x_R}\frac{\mathrm{d}\,x_R}{\mathrm{d}\,t} = -\frac{\mathrm{d}\,\lambda}{\mathrm{d}\,x_R}\dot{x}_R \tag{1}$$

The shear component of the electromagnetic forces between the two parts of the generator is denoted F_{EM}, the spring force denoted F_S, frictional forces on the armature F_{FA} and drag forces due to fluid resistance F_{DA}. All forces are defined as positive for the armature in the same direction as positive x_A. The acceleration of the armature is then given by (2), where m_A is the mass of the armature.

$$\ddot{x}_A = \frac{F_{EM} + F_S + F_{FA} + F_{DA}}{m_A} \tag{2}$$

The armature friction is calculated from the conventional equation $F_{FA} = -\operatorname{sgn}(\dot{x}_A)\mu_{fA}N$ where μ_{fA} is the coefficient of friction for the armature bearings, N is the normal force acting on the bearings and the function sgn gives sign of $\dot{x}_A$, or zero when $\dot{x}_A = 0$. The fluid drag on the armature is calculated from (3) where ρ is the density of the fluid (taken as 1.23 kg/m^3 for air and 1025 kg/m^3 for sea water), C_d is

the drag coefficient and A_n the cross-sectional area of the armature perpendicular to the direction of motion.

$$F_{DA} = -\frac{1}{2}\rho C_d A_n \dot{x}_A |\dot{x}_A| \tag{3}$$

When mounted vertically, there will also be friction between the translator and it's bearings which is dependent on the air-gap closing forces. As the two parts of the armature are fixed relative to each other these forces will tend to cancel out. The resulting force on the translator will then be due to manufacturing tolerances resulting in an unbalanced air gap on either side, and are therefore difficult to estimate in advance. For this reason, simulations in which the generator is operating as part of the WEC neglect the translator friction. However, some simulations performed for comparison with dry validation, where for practical reasons the generator is mounted horizontally, do calculate translator friction in a similar manner to the armature friction.

For simulation convenience, the machine is connected to a simple series circuit consisting of the winding resistance and inductance, and a load resistor. In practice power electronics will be required to process the output. The current in the circuit can be found by solving the differential equation obtained from nodal analysis, presented in (4), where R is the total resistance of the circuit, i.e. the combined load and coil resistance, and L is the inductance.

$$\frac{\mathrm{d}\, i(t)}{\mathrm{d}\, t} = \frac{\mathrm{EMF} - i(t)R}{L} \tag{4}$$

2.2 Hydrodynamic Model

The motion of bodies in ocean waves are commonly simulated in the frequency domain, based on Stoke's linear wave theory, [8,15], but also modelled in the time domain, originally by Cummins [5] and Jefferies [11]. Time domain simulations have been used for various types of WEC, especially where nonlinear forces operate on the buoy, typically due to the control strategy used, [2], [6] or due to a nonlinear Power Take Off (PTO) system [3].

The hydrodynamic forces operating on the buoy are the excitation, radiation and buoyancy forces. When superposed, these yield the total dynamic and static forces from the incident waves, and here are determined in both heave and surge. The translator mass is made large enough so that the tether connecting it to the buoy is prevented from becoming slack, i.e. by having a weight greater than the combined internal generator shear forces, and the PTO force is always transmitted to the heaving buoy. It is further assumed, however, that the mass of the translator is concentrated in the buoy mass for the purposes of calculating its motion.

The buoyancy force, F_{BB}, is based on Archimedes' principle, given by (5), where ρ is the density of water, g the acceleration due to gravity, r the radius of the buoy and h the buoy displacement in heave.

$$F_{\mathrm{BB}} = -\rho g \pi r^2 h \tag{5}$$

The excitation force in heave and surge (F_{BEH} and F_{BES}), is the force required to keep the buoy still when experiencing incident waves. The excitation force is a function of the amplitude, frequency and phase of the waves and the shape and the mass distribution of the buoy and depends on the current time only. The values are obtained from WAMIT [1], which is a boundary element method software, first developed by Newman's group at MIT.

The radiation force is the force required to move the buoy, and in this case the Snapper generator mass, in still water, in the same manor as it responds to incident waves. The radiation forces in heave and surge, without a component which is related to the added mass at an infinite frequency, are denoted by F_{BRH} and F_{BRS}. The general equation for the radiation force in either heave or surge is given in (6). The radiation forces are functions of the velocities of the buoy (in heave or surge) at the current and all previous time, and also the shape and mass distribution of the buoy. The radiation forces depend on the function K which is given by (7).

$$F_{\mathrm{BR}} = \int_0^t v_B K(t-\tau)\, \mathrm{d}\, t \tag{6}$$

$$K(t) = -\frac{2}{\pi}\int_0^\infty \omega \left(M_B(\omega) - M_\infty\right) \sin(\omega t)\, \mathrm{d}\, \omega \tag{7}$$

Prony's method [4,7] has been employed to reduce the computational time necessary to calculate the radiation force by evaluating $K(t)$, through equating (7) to the sum of exponential functions in (8). The values of α_n, and β_n are determined using WAMIT [1], and have different values in the heave and surge directions. A finite number of these functions provide an approximate result with an accuracy related to the number of terms used in the sum.

$$K(t) = \sum_{n=1}^{N} \alpha_n \exp(\beta_n t) \tag{8}$$

By setting $F_{BR} = \sum_{n=1}^{N} F_{\mathrm{BR}n}$, the differential of F_{BR} with respect to time is equivalent to the summation of the differentials of $F_{\mathrm{BR}n}$, which, using the mathematical technique "differentiating under the integral sign" are calculated from (9). For the simulations presented here, twenty α_n, β_n, couples have been used for both heave and surge. This number of terms have been shown to have greater than 99% accuracy compared to the direct calculation of $K(t)$ from (7).

$$\dot{F}_{\mathrm{BR}n} = \beta_n I_n + \alpha_n v_B \tag{9}$$

To get the heave and surge components of the forces, v_B in (9) and (6) is replaced with $\dot{h}$ and $\dot{s}$ where s is the buoy displacement in surge.

Fluid drag force on the heaving buoy, F_{BD}, as it moves through the water have also been included using the method presented in [10] with a buoy drag coefficient of 0.8. This drag force is only calculated in heave at present.

2.3 The Combined Model

The equation of motion for the armature was given in (2) and similarly, the equations of motion for the buoy in heave and surge are given by (10) and (11) where m_{TB} is the mass of the translator and buoy combined.

$$(m_{TB} + M_\infty)\ddot{h} = F_{BEH} + F_{BRH} + F_{BB} + F_{EMH} + F_{BD} \quad (10)$$

$$(m_{TB} + M_\infty)\ddot{s} = F_{BES} + F_{BRS} + F_{EMS} \quad (11)$$

In (10) and (11), F_{EMH} and F_{EMS} are the proportions of the electromagnetic forces from the PTO (F_{EM}) transmitted to the buoy via the tether in heave and surge, determined through simple vector algebra.

The limitations of the hydrodynamic simulation are mainly due to the failure to account for friction between some parts of the WEC (e.g. between the hawse hole and tether), the assumptions of linear wave theory, and the combination of the buoy and translator mass for the purposes of calculating the buoy accelerations. This assumption is justified on the basis that most of the buoy motion occurs in heave, and also that the translator mass, in all cases presented here, is much less than that of the buoy. The assumption of linear wave theory means that eddies, turbulence, wakes and flow separation are not incorporated into the simulation. The system of differential equations which makes up the WEC simulation has been evaluated using the built-in MATLAB® Ordinary Differential Equation (ODE) solvers.

3. Prototype Design and Simulation

A prototype system has been designed based on iterations of the simulation methods presented in the previous sections. This prototype system is to be tested in the wave dock at the National Renewable Energy Centre (Narec) in the UK and has been primarily designed to validate the simulation tools and Snapper concept. Therefore, simulations have centered around a buoy and generator suited to this wave dock, as opposed to creating a scale model of a future production device. A picture of the test rig with the generator in place is shown in Fig. 4. The armature of the generator is of length 0.5 m and the translator approximately 1.5 m. The main design considerations were the trade-off between the desired power output and the available vertical height available in the test wave tank of 7.2 m. A series of simulations in three modes of operation have been performed as an initial validation of the concept. The first of these is with an infinitely long translator moving with a proscribed motion, in this case a constant velocity of 1 ms^{-1} (Test T1). A second simulation has been performed with the full WEC system operating in single-frequency sinusoidal waves with an amplitude of 0.5 m and frequency 0.35 Hz, intentionally close to the buoy resonant frequency of around 0.4 Hz (Test T2). The final set of simulations is for the buoy operating in random waves

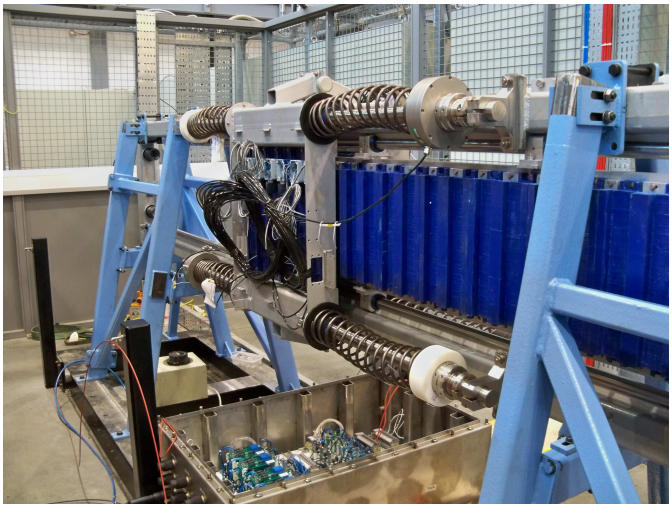

Fig. 4. The snapper generator mounted on the linear test rig.

TABLE I
SIMULATION OUTPUTS WITH LOCKED AND UNLOCKED ARMATURE.

	Locked			Not Locked		
	T1	T2	T3	T1	T2	T3
Mean Power (W)	153.06	522.86	51.10	502.58	1376.55	1.96
RMS EMF (V)	74.19	97.26	30.35	135.09	158.89	5.96
RMS Current (A)	0.38	0.50	0.15	0.69	0.80	0.03
Peak EMF (V)	102.19	210.84	97.13	467.90	628.13	76.63
Peak Current (A)	0.52	1.09	0.50	2.38	3.14	0.40

generated using a PM Spectrum, also with peak frequency 0.35 Hz (Test T3). The buoy used in these simulations is a cylinder of diameter 2 m and draft 1 m.

Simulations T1, T2 and T3 have been performed with the generator operating with the armature free to move, i.e. normal operation, and also with the armature locked in place, acting as a conventional linear generator. A summary of some important outputs from each of these tests is shown in Table I. As a further comparison, results from a third set of simulations with the armature locked, and the grid resistance reduced to yield a similar rms current for the duration of the simulations are also presented in Table II. These show that the power output is increased in snapping mode even if we operate the machine armature with similar thermal loading when locked. The mean powers reported in all cases in this paper are the power dissipated in the load resistor R_{grid}.

The fixed speed simulation results are based on 60 seconds

TABLE II
SIMULATION OUTPUTS WITH LOCKED ARMATURE AND REDUCED OUTPUT RESISTANCE.

	T1	T2	T3
Mean Power (W)	241.17	810.11	84.06
RMS EMF (V)	74.33	96.75	31.02
RMS Current (A)	0.64	0.83	0.27
Peak EMF (V)	102.19	206.20	96.11
Peak Current (A)	0.89	1.78	0.83

of operation, while the single frequency wave simulations and random wave simulations were run for 120 and 500 seconds respectively. Simulation of the full system has been based on a water depth of 7.2 m (the wave tank depth) and the random waves used in T3 are based on 100 frequencies evenly spaced in the range 0.167 Hz to 2 Hz. This range of frequencies was again chosen for suitability for testing in the wave tank rather than offering an indication of the WEC's performance in a real sea. Future designs will use seas more indicative of the real conditions that would be experienced.

It can also be seen that in test T3, the snapping design produces virtually no power. This is a result of a mismatch between the chosen spring constant and the incoming waves which results in the armature simply oscillating in time with the translator without snapping. If we double the amplitude of the incoming waves the sprung mode exports mean a power of 331 W, the locked armature mode 163 W and the locked armature with reduced output resistance 256 W.

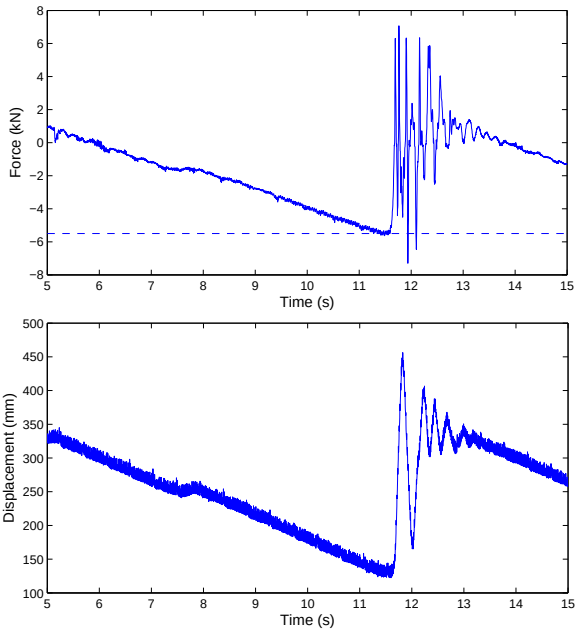

Fig. 5. Forces reported by translator load cell (top) and displacement of armature (bottom) during a single snapping event. The dashed line in the top figure marks a value of -5.5 kN on the y-axis as a visual aid.

4. Prototype Generator Test Results

The generator design for the prototype system described in Section 3 has been built and undergone dry testing prior to its deployment in a wave tank. The generator has been mounted in a frame and driven by a ball and screw drive using the CAM mode from Control Techniques' Advanced Position Control. The displacements shown here have been recorded from linear transducers rather than derived from the applied drive profile.

A number of tests have been performed in order to validate the generator model and inform future designs. The peak force experienced just prior to the snap is approximately 5.5 kN, as shown in Fig. 5. The predicted peak force from the FEA simulations is around 4.0 kN. There are several possible reasons for this deviation in the force from the predicted values such as variation in the size of the armature magnets (a 1-2 mm difference is sufficient to increase the forces by this amount), specific aspects of the construction of the physical device, an inadequacy of the 2D FEA to capture all of the behavior of the 3D system, or the significance of end effects which have not been included. The forces shown in Fig. 5 are recorded from a calibrated load cell fitted to the translator drive, and will therefore include additional forces, such as translator friction etc. It can also be seen that higher forces are observed immediately after a snapping event despite the coils being disconnected from any circuit. This indicates some additional losses may be taking place, possibly due to eddy currents in either the armature and translator.

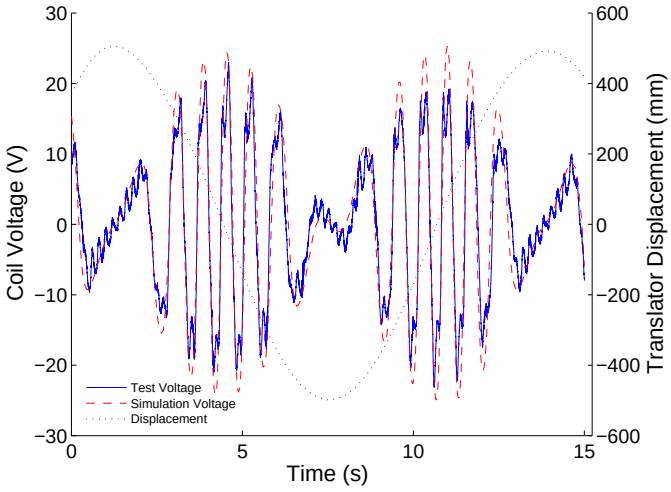

Fig. 6. Comparison of the simulation and actual test voltage with the armature locked in place.

Fig. 6 shows the open circuit voltage of a single coil when operating with the armature locked in place, with the predicted voltage from the simulation operating with the same prescribed motion. A DC bias in the test measurements of the voltage has been removed by subtracting the mean value of the voltage from the test results. Despite the noise present in the test measurements it is possible to see that the simulation predicts the voltage quite well in this case, although it is of slightly lower than predicted amplitude. The predicted and actual voltage during a single snapping event is shown in Fig. 7. The snapping event was performed by moving the translator at a constant speed of approximately 0.04 ms^{-1} (the jog speed of the test rig drive). The simulation results are based on a coefficient of friction for the armature of 0.4.

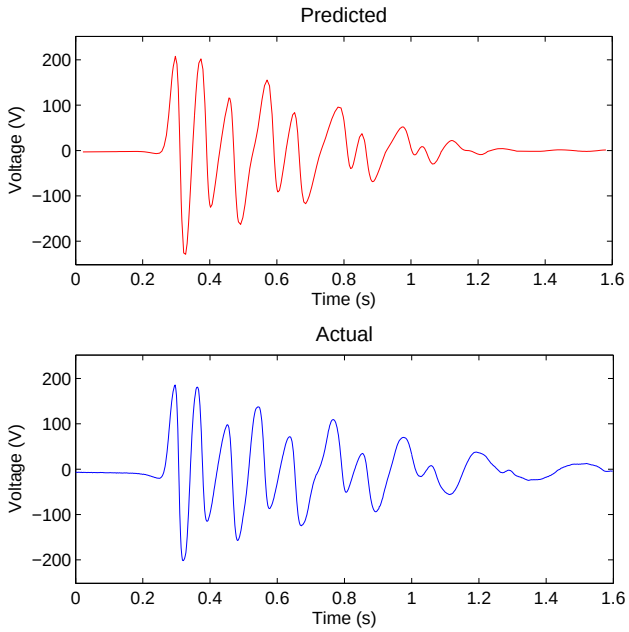

Fig. 7. Simulated and measured test voltage during single snapping event.

5. Discussion

The results presented here give some confidence in the electromechanical simulation of the generator system, however, further work is required to determine the reasons for the discrepancy in the predicted and observed forces. Additional tests are to be performed which will aid in this analysis by testing the armature and translator frictional forces with the armature magnets removed.

The implications of the simulation results presented in Section 3 should not be overstated. Although higher power output is achieved for this particular machine design when operating with the snapping action, when compared to operation with a locked armature, the authors recognise that this does not prove that every possible direct-drive machine design would benefit from this technology. However, these results do show that further investigation is warranted. The full WEC system will be tested in the wave tank at Narec in July 2011.

6. Conclusions

A combined hydrodynamic and electromechanical simulation of a WEC based on a direct-drive linear generator incorporating a snapping magnetic coupling has been presented. The incoming wave energy is stored in a spring until the magnetic coupling force is exceeded and the energy is converted to electrical energy in a short pulse. The combined simulation is based in the time domain and makes use of precomputed hydrodynamic coefficients and forces to determine the wave forces acting on a heaving buoy. Simulations demonstrating an increased average power output to the grid for one particular machine design have been presented, to to demonstrate the validity of the concept. A comparison of the predicted and recorded test values of the electromechanical simulation of the generator component show reasonable agreement.

Acknowledgment

The Snapper project and the research carried out during the project has received funding from the European CommunitySs Seventh Framework Programme (FP7: 2007-2013) under grant agreement number: 232099. The authors would like to gratefully acknowledge the support of the European Community.

The authors would also like to thank the Snapper Consortium for their support on this project.

References

[1] *WAMIT user manual version 6.0, 6.0PC, 5.3S*. WAMIT Inc.

[2] A. Babarit and A. H. Clément. Otpimal latching control of a wave energy converter. In *6th European Wave and Tidal Energy Conference EWTEC*, page 19Ű26, 2005.

[3] H. Bailey. *Influence of a nonlinear Power Take Off on a Wave Energy Converter*. PhD thesis, The University of Edinburgh, 2010.

[4] H. Bailey and I. G. Bryden. Influence of a quadratic power take off on the behaviour of a self contained inertial referenced wave energy converter. *Proceedings of the Institution of Mechanical Engineers, Part M: Journal of Engineering for the Maritime Environment*. Accepted for publication in 2011.

[5] W. E. Cummins. The impulse response function and ship motions. *Schiffstechnik*, page 491Ű502, 1962.

[6] A. F. de O. Falcão. Modelling and control of oscillating-body wave energy converters with hydraulic power take-off and gas accumulator. *Ocean Engineering*, 34(14-15):2021 – 2032, 2007.

[7] G. Duclos, A. H. Clément, and G. Chatry. Absorption of outgoing waves in a numerical wave tank using a self adaptive boundary condition. *Int J Offshore Polar Engng*, 11(3):168–175, 2001.

[8] J. Falnes. *Ocean Waves and Oscillating Systems, Linear interactions including wave-energy extraction*. Cambridge University Press, 1 edition, 2002.

[9] J. Falnes. A review of wave-energy extraction. *Marine Structures*, 20(4):185 – 201, 2007.

[10] A. Grilli, J. Merrill, S. Grilli, M. Spaulding, and J. Cheung. Experimental and numerical study of spar buoy-magnet/spring oscillators used as wave energy absorbers. In *Proceedings of the Seventeenth (2007) International Offshore and Polar Engineering Conference*, pages 489–496. Citeseer, 2007.

[11] E. Jefferys. Simulation of wave power devices. *Applied Ocean Research*, 6(1):31 – 39, 1984.

[12] M. Leijon, H. Bernhoff, O. Agren, J. Isberg, J. Sundberg, M. Berg, K. Karlsson, and A. Wolfbrandt. Multiphysics simulation of wave energy to electric energy conversion by permanent magnet linear generator. *Energy Conversion, IEEE Transactions on*, 20(1):219–224, 2005.

[13] M. A. Mueller and N. J. Baker. Direct drive electrical power take-off for offshore marine energy converters. *Proceedings of the I MECH E Part A Journal of Power and Energy*, 219(3):223–234, 2005. doi:10.1243/095765005X7574.

[14] H. Polinder, M. Damen, and F. Gardner. Linear PM Generator System for Wave Energy Conversion in the AWS. *IEEE Transactions on Energy Conversion*, 19(3):583–589, Sept. 2004.

[15] T. Sarpkaya and M. Isaacson. *Mechanics of Wave Forces on Offshore Structures*. Van Nostrand Reinhold Company, 1981.

[16] R. Waters, M. StaÌŁlberg, O. Danielsson, O. Svensson, S. Gustafsson, E. StroÌĹmstedt, M. Eriksson, J. Sundberg, and M. Leijon. Experimental results from sea trials of an offshore wave energy system. *Applied Physics Letters*, 90(3):034105, 2007.